Sensors and Materials, Vol. 32, No. 7 (2020) 2433–2441
MYU Tokyo

S & M 2272

Fabrication and Thermoelectric Properties of Chromium Silicide Thin Films

Takao Mori,[1,2*] Takashi Aizawa,[1] S. N. Vijayaraghavan,[1] and Naoki Sato[1]

[1]WPI-MANA and CFSN, National Institute for Materials Science (NIMS), Namiki 1-1, Tsukuba 305-0044, Japan
[2]Graduate School of Pure and Applied Sciences, University of Tsukuba, 1-1-1 Tennoudai, Tsukuba 305-8671, Japan

(Received March 30, 2020; accepted May 15, 2020)

Keywords: thermoelectric, thin film, magnetic semiconductor, power factor, thermal conductivity

Thermoelectric thin films are candidate materials that can be used to supply the energy harvested to autonomously power Internet of Things (IoT) sensors and devices. This work deals with the fabrication of chromium silicide thin films and the characterization of their thermoelectric properties. The films were grown by utilizing a high-temperature molecular beam epitaxy (MBE) apparatus under different conditions. The highest power factor of more than 0.6 mW/m K^2 was obtained for the chromium silicide film deposited at a temperature of 900 °C. The thermal conductivity of the thin film was observed to be approximately one-third that of bulk $CrSi_2$.

1. Introduction

The application of thermoelectric power generation has still not been realized in a large market. In addition to the performance of power generation, cost has also been a big problem. One promising application that has gained interest is thermal energy harvesting to dynamically power innumerable Internet of Things (IoT) sensors and devices.[1,2] In this case, the maintenance-free possibility of thermoelectrics is attractive, because changing batteries for a huge number of sensors and devices is not feasible. It is therefore important for IoT applications to find methods appropriate for processing and fabricating modules for high-performance materials. The use of inorganic thermoelectric thin films is one possibility.

The performance of thermoelectric materials is determined by their figure of merit:

$$ZT = \alpha^2 \sigma \kappa^{-1} T, \tag{1}$$

where $\alpha^2\sigma$ is the power factor, and the conversion efficiency is a function of ZT. To achieve high ZT, a high electrical conductivity σ, but a low thermal conductivity κ, and a large Seebeck coefficient α, but a high σ, are required. Therefore, there are some obvious paradoxes and trade-offs in the requirements of the physical properties of materials to achieve high thermoelectric performance. There have been several good overall reviews of recent advancements in enhancing the ZT of thermoelectric materials.[3,4]

*Corresponding author: e-mail: MORI.Takao@nims.go.jp
https://doi.org/10.18494/SAM.2020.2889

ISSN 0914-4935

We have proposed the use of magnetism to enhance the properties of thermoelectric materials. Magnetic ion doping has been demonstrated for various systems, such as $CuGaTe_2$,[5] Bi_2Te_3,[6] and SnSe,[7] to be a possible route to increase the power factor. Such an increase is not automatic and occurs in cases where electrical carriers have strong coupling with doped magnetic moments, effectively modifying transport properties. Namely, this interaction "drags" the carriers, leading to an increase in effective mass that in turn increases the Seebeck coefficient. This will be detrimental to mobility, but the overall increase in power factor has been realized.[5–7] Some good-performance thermoelectric compounds have also been recently discovered amongst magnetic semiconductors, where magnetic elements are the main constituents.[8–13] Carrier-doped $CuFeS_2$ exhibits a large power factor at room temperature (RT), speculated to originate from strong magnetic interactions.[8] Theoretical calculations have also shown that $CuFeS_2$ has an antiferromagnetic configuration, resulting in the largest Seebeck coefficient and power factor.[9] At low temperatures, the contribution of carrier–magnon interactions to the Seebeck coefficient was also indicated.[10] Sulfides with a spinel structure, i.e., thiospinels, were generally observed to have poor thermoelectric properties.[14] Good thermoelectric properties of $ZT = 0.43$ were revealed in $CuCr_2S_4$ by tuning the carrier concentration by Sb doping, whereby the intrinsic properties of a magnetic system with a relatively large effective mass were manifested at relatively large power factors.[11] Cr_2Se is another magnetic system with a relatively good thermoelectric performance near RT, and importantly, p, n tuning is possible without external element doping.[12] In the Heusler alloy Fe_2VAl system, where itinerant weak ferromagnetic behavior was engendered by doping, spin fluctuation was found to increase the Seebeck coefficient, for example by 50% at 400 K.[13] Ultrahigh performance at $ZT > 4$ has also been reported in related Heusler films.[15] Inorganic thermoelectric thin films have been fabricated and investigated for various material systems,[16] for example, thermoelectric thin films of oxides,[17,18] borides,[19,20] and stannides.[21]

Here, we report on the fabrication and thermoelectric properties of chromium silicide thin films. Chromium silicide is of interest for us, because for its future outlook, as a magnetic system[22] with high potentials as described above, and the thermoelectric properties of bulk $CrSi_2$ were investigated previously.[23,24] A relatively large power factor of ~1 mW/m K^2 has been reported for a pure bulk material at RT.[24] Nakasawa *et al.* succeeded in increasing this to ~1.4 mW/m K^2 at RT via Mo doping.[25] The reported high thermal conductivity of 12 W/m K at RT for the bulk material[25] also makes it an attractive system that could benefit from being formatted into the thin film form. These are the reasons why we have focused on the chromium silicide system in our investigations of the fabrication of thin films and their thermoelectric properties.

2. Materials and Methods

Chromium silicide thin films were deposited on sapphire (0001) substrates (Shinkosha Co., Ltd.) using a molecular beam epitaxy (MBE; EV-500, Eiko Co., Ltd.) apparatus. Each sapphire substrate was degas-heated at 1000 °C for 1 h in vacuum before film deposition. Si and Cr were evaporated using special high-temperature K-cells, namely, MB-3000Si (Eiko Co., Ltd.) with a

Ta crucible for Si and TUBO-e (CreaTec Fischer & Co., GmbH) with a vitreous carbon crucible for Cr, respectively. The deposition conditions are listed in Table 1. As common conditions, the growth time was 90 min, and the heating temperature of the Cr cell was 1150 °C. The film thickness was measured using a stylus profilometer (Dektak 6M, Bruker). The crystal structure was evaluated by X-ray diffraction (XRD), using a powder diffractometer (SmartLab 3, Rigaku Corp.).

The thermoelectric properties of the deposited thin films were measured using ZEM-3 (ULVAC). The cross-plane thermal conductivity was evaluated using a customized focused picosecond time-domain thermoreflectance (TD-TR) instrument (PicoTR, Picotherm Corp.) in a front-heating/front-detection configuration.[26–28] A 100-nm-thick Pt thin film was deposited on chromium silicide thin film surfaces using a DC sputtering system to detect transient temperature changes. A 1550 nm infrared pulsed laser with a repetition frequency of 20 MHz and a pulse duration of 0.5 ps was used as a heat source. A 780 nm probe laser was used to detect thermoreflectance signals. Here, we assumed the specific heat of all films as 3R from the Dulong–Petit law (0.575 J g^{-1} K^{-1}) for the calculation of the thermal conductivity.

3. Results and Discussion

Figures 1 and 2 show the XRD patterns of the MBE-grown chromium silicide thin films. As summarized in Table 1, various thin films were obtained under different thin film growth conditions.

The substrate temperatures of RT and 400 °C were apparently too low to achieve chromium silicide film growth, and phases were obtained from 600 °C and above. For substrate heating temperatures of 600 and 800 °C, the majority phase was the CrSi metallic phase with significant $CrSi_2$ growth. For 900 and 1000 °C substrate heating, $CrSi_2$ was obtained as the majority phase, with CrSi and Cr_5Si_3 as minority phases.

In an attempt to reduce the amount of the metallic CrSi phase and relatively increase the amount of the main $CrSi_2$ phase, the Si cell was heated up to 1525 °C. As can be observed in

Table 1
Chromium silicide film growth parameters and phases.

Sample ID	Substrate temp. (°C)	Si cell temp. (°C)	Thickness (nm)	Majority phase	Minority phases
RT	RT	1500	—	—	—
400	400	1500	—	—	—
600 deg	600	1500	98.3	CrSi	$CrSi_2$
800 deg	800	1500	134.9	CrSi	$CrSi_2$, Cr_5Si_3
900 deg	900	1500	134.0	$CrSi_2$	CrSi, Cr_5Si_3
1000 deg	1000	1500	106.6	$CrSi_2$	CrSi, Cr_5Si_3
600/1525 deg	600	1525	107.1	$CrSi_2$	CrSi
800/1525 deg	800	1525	—	$CrSi_2$	CrSi, Cr_5Si_3
900/1525 deg	900	1525	132.0	$CrSi_2$	CrSi, Cr_5Si_3
1000/1525 deg	1000	1525	115.0	$CrSi_2$	CrSi, Cr_5Si_3

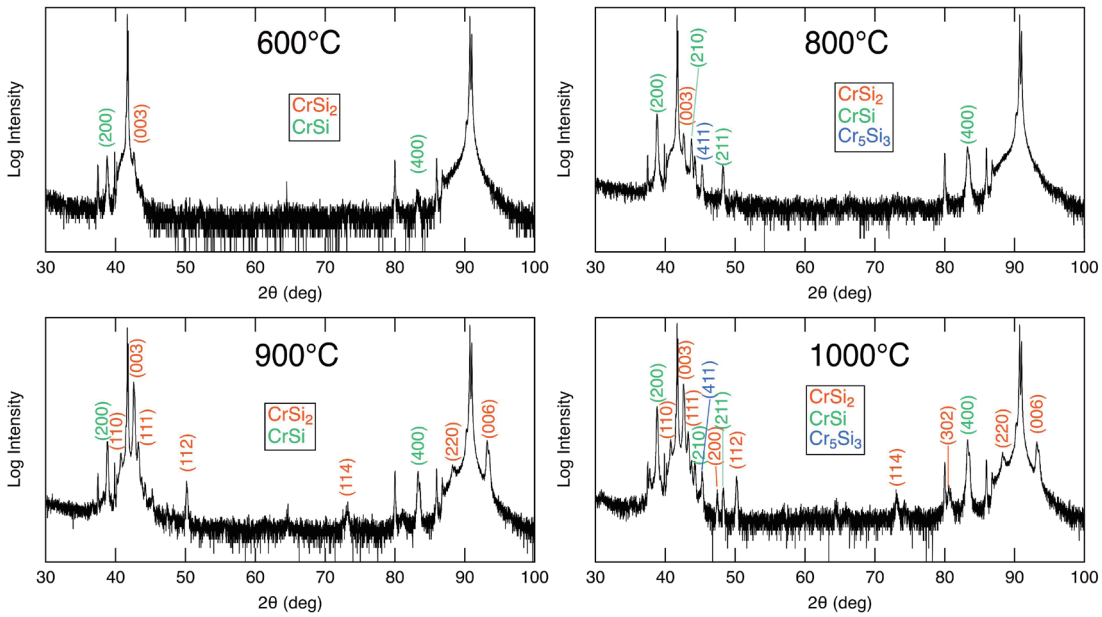

Fig. 1. (Color online) XRD patterns of chromium silicide thin films with 1500 °C Si cell heating. The indicated temperatures are the substrate heating temperatures.

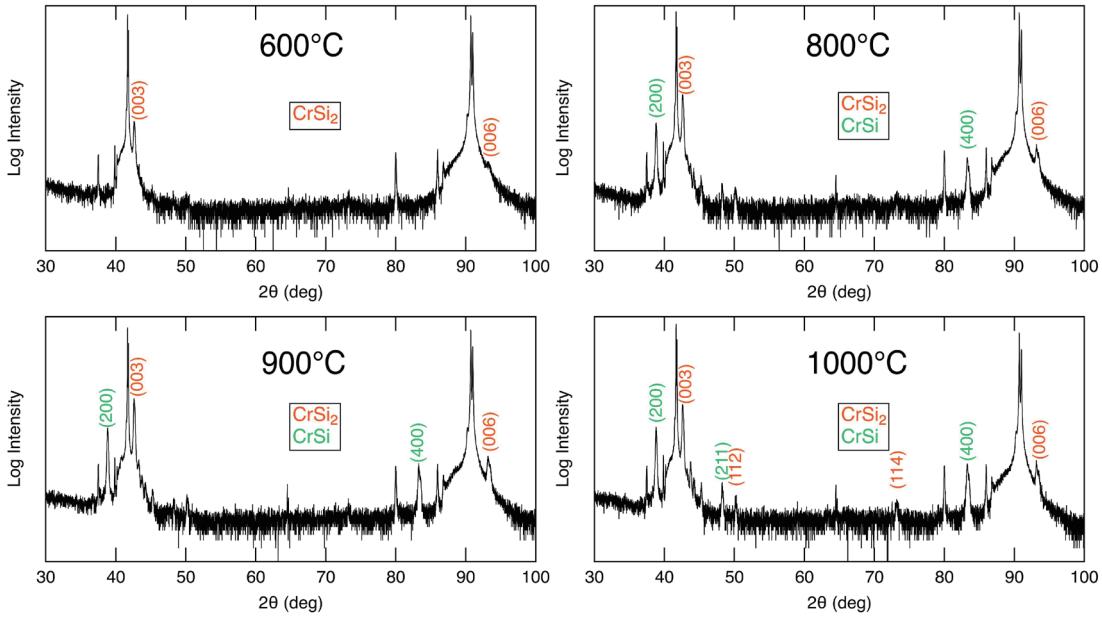

Fig. 2. (Color online) XRD patterns of chromium silicide thin films with 1525 °C Si cell heating. The indicated temperatures are the substrate heating temperatures.

Fig. 2, this did not result in a relative reduction in the amount of the CrSi phase. Apparently, the opposite behavior was observed and the thermoelectric properties subsequently degraded. Namely, the power factor of the best sample in this series was around half that of Si heated

at 1500 °C. The tantalum material of our Si cell might have reacted with Si at higher temperatures, and it was not easy to tune the conditions further to optimize the $CrSi_2$ MBE thin film growth on our apparatus. This should be examined in future attempts together with doping to tune the properties.

The thermoelectric properties of the chromium silicide thin films, namely, the Seebeck coefficient, resistivity, and power factor, are shown in Fig. 3. The Seebeck coefficient of the 900 deg film with substrate heating is larger than 140 μV/K near RT, slightly smaller but similar in magnitude to what was previously reported for bulk $CrSi_2$.[24] This can be considered to be the effect of the metallic CrSi minority phase. Reductions in the electrical conductivities and power factors of thin films of various thermoelectric materials compared

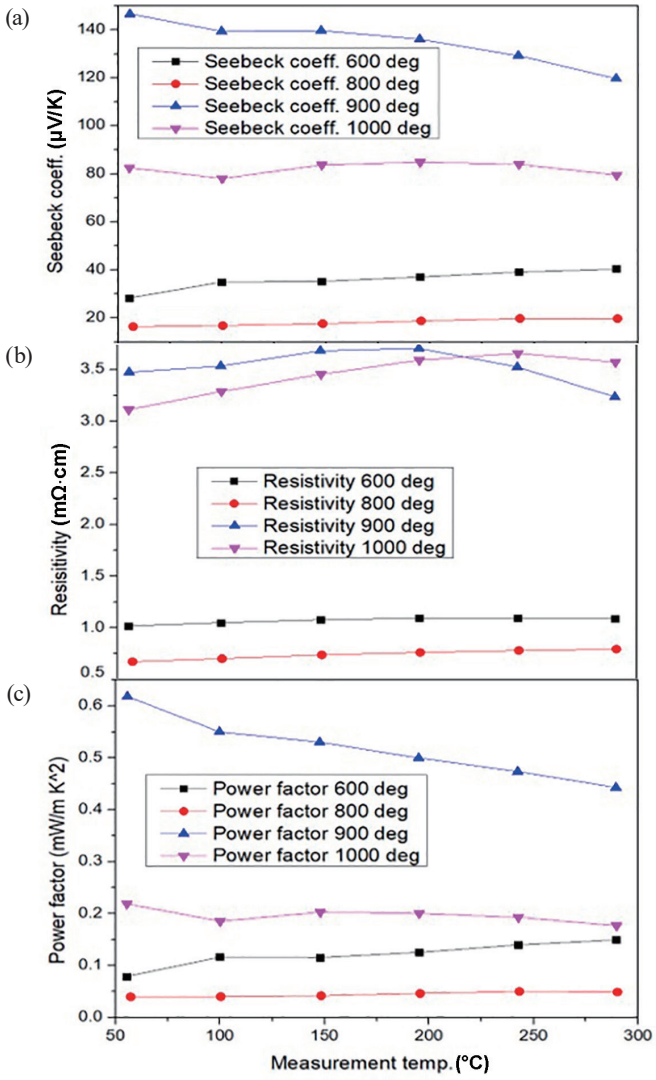

Fig. 3. (Color online) Thermoelectric properties: (a) Seebeck coefficient, (b) resistivity, and (c) power factor.

with the bulk material, have typically been observed.[16] The difference in polycrystalline quality between bulk samples and thin films can be a typical origin of this behavior, but the Seebeck coefficient is not affected. The 600 and 800 deg films with relatively high contents of metallic CrSi exhibit lower resistivities and smaller Seebeck coefficients. Metallic minority phases were previously observed in some cases to markedly increase the electrical conductivity and power factor;[29] however, in this case, even with this possible benefit, the 900 deg thin film exhibits a higher resistivity than the bulk, which is likely due to the detrimental thin-film effect mentioned previously. Although there is an apparatus limitation at present as discussed above, if we can finely tune the amount of the metallic CrSi phase in $CrSi_2$ films, this can lead to the enhancement of the overall power factor. Such a metallic minority phase can generate a nonpercolating metallic partial network in the material, which will not markedly degrade the Seebeck coefficient, while enhancing the electrical conductivity significantly.[29]

The best power factor of the presently obtained chromium silicide films is ~0.6 mW/m K^2 near RT obtained for the 900 deg thin film. This is smaller than ~1 mW/m K^2 reported for bulk $CrSi_2$, but for thermoelectric thin films with abundant elements, it is a relatively large value at RT.[17–21]

A significant increase in power factor to ~1.4 mW/m K^2 at RT was previously reported for Mo-doped bulk $CrSi_2$, and doping experiments should be carried out in future studies. Furthermore, as mentioned in the introduction, the increase in the power factor has been achieved by considering magnetism,[5–9] and as a future outlook, this possibility should also be investigated for chromium silicide thin films.

The behavior of the series of films with 1525 °C Si cell heating is as expected, with lower Seebeck coefficients due to the relatively higher content of metallic CrSi (Fig. 4). The maximum power factor obtained for the 1000/1525 deg film is only around half that of the 1500 °C Si cell heating series.

The determined thermal conductivities of the selected thin film samples are listed in Table 2. The electronic thermal conductivity was determined using the Wiedemann–Franz law, where $\kappa_E = L\sigma T$. 2.44×10^{-8} V^2/K^2 was used as the Lorenz number L here. κ_E is relatively small, and it can be observed that the major part of thermal conductivity is the lattice thermal conductivity.

The thermal conductivity of bulk $CrSi_2$ has been reported as 12 W/m K at 300 K.[25] Compared with the highest power factor film 900 deg sample, there is an approximately one-third reduction in thermal conductivity. The metallic CrSi minority phase is difficult to qualitatively gauge, since it can have opposite effects, namely, the thermal conductivity decreases via interfaces, but it also increases via highly conductive channels. In any case, all the chromium silicide films synthesized under standard conditions exhibited a lower thermal conductivity than bulk $CrSi_2$, so the thin-film format is effective in reducing the thermal conductivity.

We consider other possible effects of the differences in the thickness between the thin films, from 98.3 nm to 134.9 nm, on the thermoelectric properties measured. The measurements themselves should not have any effect. Regarding the intrinsic properties, even for the thinnest film, in this range we do not expect any specific electronic effects that are not observed in

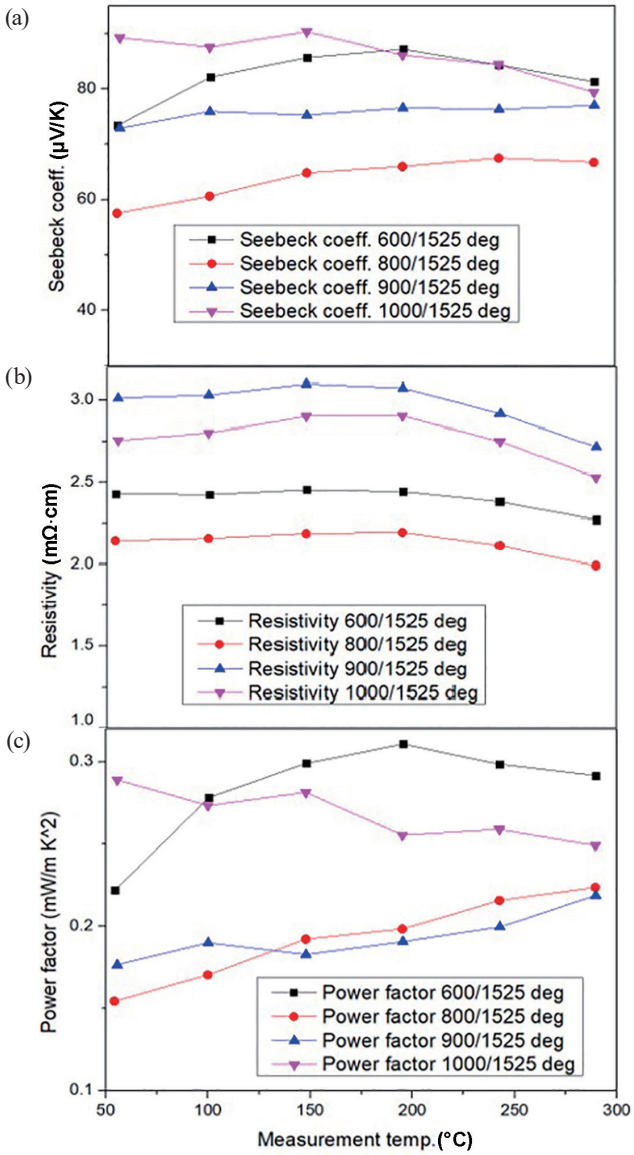

Fig. 4. (Color online) Thermoelectric properties: (a) Seebeck coefficient, (b) resistivity, and (c) power factor.

Table 2
Thermal conductivities of chromium silicide films.

Sample ID	Thermal diffusivity at 300 K (10^{-6} m^2/s)	Thermal conductivity κ at 300 K (W/mK)	Electronic thermal conductivity κ_E at 323 K (W/mK)
600 deg	2.85	7.20	0.79
800 deg	4.05	10.23	1.19
900 deg	3.33	8.40	0.23
1000 deg	3.01	7.61	0.26
600/1525 deg	2.73	6.90	—
900/1525 deg	3.65	9.22	—
1000/1525 deg	3.54	8.95	—

the bulk form, such as quantum confinement or electronic structure modulation. However, according to a previous report on the theoretical evaluation of the thermal conductivity of $CrSi_2$,[30] phonons with a mean free path of about 100 nm do not have significant contributions to thermal transport. Therefore, the differences in the thickness between our samples are not expected to have any effect on the thermoelectric properties.

4. Conclusions

We fabricated chromium silicide thin films by MBE. The film with the highest thermoelectrical performance had $CrSi_2$ as the main phase. The highest power factor of more than 0.6 mW/m K^2 at RT was obtained for the chromium silicide film with a deposition temperature of 900 °C and a Si cell heating temperature of 1500 °C. For thermoelectric thin films with abundant elements, the obtained power factor was relatively large, which made the thin films promising systems to be investigated further. These thin films exhibited a thermal conductivity that was approximately one-third that of bulk $CrSi_2$. Bulk $CrSi_2$ exhibited significant increases in power factor via doping; this should also be further examined in the fabricated thin films, together with an investigation on any correlation with magnetic properties, and their tuning.

Acknowledgments

This work was supported by Japan Science and Technology Agency (JST), Mirai Program Grant Number JPMJMI19A1, CREST JPMJCR19Q4, and JSPS KAKENHI Grant Number JP17H02749 and JP16H06441.

References

1 T. Mori and S. Priya: MRS Bull. **43** (2018) 176. https://doi.org/10.1557/mrs.2018.32
2 I. Petsagkourakis, K. Tybrandt, X. Crispin, I. Ohkubo, N. Satoh, and T. Mori: Sci. Tech. Adv. Mater. **19** (2018) 836. https://doi.org/10.1080/14686996.2018.1530938
3 J. Mao, Z. Liu, J. Zhou, H. Zhu, Q. Zhang, G. Chen, and Z. Ren: Adv. Phy. **67** (2018) 69. https://doi.org/10.1080/00018732.2018.1551715
4 T. Mori: Small **13** (2017) 1702013. https://doi.org/10.1002/smll.201702013
5 F. Ahmed, N. Tsujii, and T. Mori: J. Mater. Chem., A. **5** (2017) 7545. https://doi.org/10.1039/C6TA11120C
6 S. Acharya, S. Anwar, T. Mori, and A. Soni: J. Mater. Chem. C. **6** (2018) 6489. https://doi.org/10.1039/c8tc00788h
7 J. B. Vaney, S. A. Yamini, H. Takaki, K. Kobayashi, N. Kobayashi, and T. Mori: Mater. Today Phys. **9** (2019) 100090. https://doi.org/10.1016/j.mtphys.2019.03.004
8 N. Tsujii and T. Mori: Appl. Phys. Exp. **6** (2013) 043001. https://doi.org/10.7567/APEX.6.043001
9 H. Takaki, K. Kobayashi, M. Shimono, N. Kobayashi, K. Hirose, N. Tsujii, and T. Mori: Mater. Today Phys. **3** (2017) 85. https://doi.org/10.1016/j.mtphys.2017.12.006
10 R. Ang, A. U. Khan, N. Tsujii, K. Takai, R. Nakamura, and T. Mori: Angew. Chem. Int. Ed. **54** (2015) 12909. https://doi.org/10.1002/anie.201505517
11 A. U. Khan, R. A. R. A. Orabi, A. Pakdel, J. B. Vaney, B. Fontaine, R. Gautier, J. F. Halet, S. Mitani, and T. Mori: Chem. Mater. **29** (2017) 2988. https://doi.org/10.1021/acs.chemmater.6b05344
12 Q. Guo, D. Berthebaud, J. Ueda, S. Tanabe, A. Miyoshi, K. Maeda, and T. Mori: J. Mater. Chem. C. **7** (2019) 8269. https://doi.org/10.1039/c9tc01634a
13 N. Tsujii, A. Nishide, J. Hayakawa, and T. Mori: Sci. Adv. **5** (2019) eaat5935. https://doi.org/10.1126/sciadv.aat5935

14 G. J. Snyder, T. Caillat, and J. P. Fleurial: MRS Proc. (MRS, 2000) Z3.3. https://doi.org/10.1557/PROC-626-Z3.3
15 B. Hinterleitner, I. Knapp, M. Poneder, Yongpeng Shi, H. Müller, G. Eguchi, C. Eisenmenger-Sittner, M. Stöger-Pollach, Y. Kakefuda, N. Kawamoto, Q. Guo, T. Baba, T. Mori, Sami Ullah, Xing-Qiu Chen, and E. Bauer: Nature **576** (2019) 85. https://doi.org/10.1038/s41586-019-1751-9
16 P. Mele, D. Narducci, M. Ohta, K. Biswas, J. Morante, S. Saini, and T. Endo: Thermoelectric Thin Films Materials and Devices (Springer, 2019). https://doi.org/10.1007/978-3-030-20043-5
17 P. Mele, S. Saini, H. Honda, K. Matsumoto, K. Miyazaki, H. Hagino, and A. Ichinose: Appl. Phys. Lett. **102** (2013) 253903. https://doi.org/10.1063/1.4812401
18 Y. Hirose, M. Tsuchii, K. Shigematsu, Y. Kakefuda, T. Mori, and T. Hasegawa: Appl. Phys. Lett. **114** (2019) 193903. https://doi.org/10.1063/1.5089679
19 S. Ghamaty, J. C. Bass, and N. B. Elsner, and edited by D. M. Rowe: Thermoelectrics Handbook, Micro to Nano (Taylor & Francis, London, 2006) p. 57.
20 G. P. L. Guélou, M. Martirossyan, K. Ogata, I. Ohkubo, Y. Kakefuda, N. Kawamoto, Y. Kitagawa, J. Ueda, S. Tanabe, K. Maeda, K. Nakamura, T. Aizawa, and T. Mori: Materialia **1** (2018) 244. https://doi.org/10.1016/j.mtla.2018.06.003
21 T. Aizawa, I. Ohkubo, M. Lima, T. Sakurai, and T. Mori: J. Vac. Sci. Technol. A. **37** (2019) 061513. https://doi.org/10.1116/1.5122844
22 D. J. Singh and D. Parker: Sci. Rep. **3** (2013) 3517. https://doi.org/10.1038/srep03517
23 I. Nishida: J. Mater. Sci. **7** (1972) 1119. https://doi.org/10.1007/BF00550193
24 T. Dasgupta, J. Etourneau, B. Chevalier, S. F. Matar, and A. M. Umarji: J. Appl. Phys. **103** (2008) 113516. https://doi.org/10.1063/1.2917347
25 H. Nakasawa, T. Takamatsu, Y. Iijima, K. Hayashi, and Y. Miyazaki, Trans. Mater. Res. Soc. Jpn. **43** (2018) 85. https://doi.org/10.14723/tmrsj.43.85
26 Y. Kakefuda, K. Yubuta, T. Shishido, A. Yoshikawa, S. Okada, H. Ogino, N. Kawamoto, T. Baba, and T. Mori: APL Mater. **5** (2017) 126103. https://doi.org/10.1063/1.5005869
27 M. Piotrowski, M. Franco, V. Sousa, J. Rodrigues, F. L. Deepak, Y. Kakefuda, T. Baba, N. Kawamoto, B. Owens-Baird, P. Alpuim, K. Kovnir, T. Mori, and Y. V. Kolenko: J. Phys. Chem. C **122** (2018) 27127. https://doi.org/10.1021/acs.jpcc.8b04104
28 R. Daou, F. Pawula, O. Lebedev, D. Berthebaud, S. Hebert, A. Maignan, Y. Kakefuda, and T. Mori: Phys. Rev. B: Condens. Matter **99** (2019) 085422. https://doi.org/10.1103/PhysRevB.99.085422
29 T. Mori and T. Hara: Scripta Mater. **111** (2016) 44. https://doi.org/10.1016/j.scriptamat.2015.09.010
30 H. Nakasawa, K. Hayashi, T. Takamatsu, and Y. Miyazaki, J. Appl. Phys. **126** (2019) 025105. https://doi.org/10.1063/1.5096458